

be difficult to obtain by routine clinical echocardiography, because RVEF cannot be measured precisely [15]. Furthermore, assessment of LVEF by routine echocardiography is sometimes difficult especially in obese patients, and patients with pulmonary disease, because precise definition of the endocardial borders is required. Recordings of the tricuspid and mitral annular motion have the practical advantages that they are relatively independent of image quality [18] and are easily done with low (<10 %) inter and intra-operator variability [19].

S_T/S_M ratio can be a noninvasive index of the relation between RV and LV filling pressure. Eq. 1 is rewritten as follows:

$$\text{CVP/PCWP} = 1/(\alpha \cdot S_T/S_M) \quad (11)$$

The relation between S_T/S_M ratio and CVP/PCWP ratio in the 243 datasets (Table 1) indeed tightly approximated a reciprocal function ($\text{CVP/PCWP} = 0.7/(S_T/S_M)$, $R^2 = 0.7$, data not shown), indicating that S_T/S_M ratio and CVP/PCWP ratio are closely related in accordance with our theoretical analysis (see “Materials and methods”). More importantly, S_T/S_M ratio may be used as a noninvasive prognosticator of HF patients. Drazner et al. [35] reported that the ratio of right atrial pressure to PCWP is associated with a risk of adverse outcomes in patients with advanced HF.

Clinical implications

The use of $\text{CVP} \cdot S_T/S_M$ may obviate the need for the pulmonary artery catheterization, which has approximately twice as many catheter-related complications (predominantly arrhythmia) as the central venous catheterization [2]. CVP alone may be useful for serial assessment of changes in PCWP. However, the accuracy of CVP for a single time-point prediction of PCWP is moderate and inferior to that of $\text{CVP} \cdot S_T/S_M$ (Fig. 3e, f). A study in heart transplant candidates showed an increase in proportion of patients with elevated filling pressures demonstrating discordance between RV and LV filling pressures [11], which suggests a potential increase in the necessity of using $\text{CVP} \cdot S_T/S_M$ rather than CVP for reliable prediction of PCWP in the management of patients with advanced HF.

The data of $\text{PVP} \cdot S_T/S_M$ may be acquired even in the outpatient clinic, since PVP can be easily and safely measured by manometry via peripheral venipuncture [22]. In today’s clinical practice, PVP is seldom measured. However, the manometric PVP measurements were commonly done until the 1970s in patients suspected of having HF [22]. Although the data of E/E_a are noninvasively obtained, the diagnostic accuracy of E/E_a for the prediction of abnormal elevation of PCWP is moderate and, overall, inferior to that of $\text{PVP} \cdot S_T/S_M$ (Fig. 4e, f). Furthermore,

correlation analysis between $\Delta E/E_a$ and ΔPCWP (Fig. 4d), and ROC analysis for E/E_a to predict ΔPCWP (Fig. 4g, h) indicates that E/E_a has poor diagnostic accuracy in tracking changes in PCWP, which was also reported in previous clinical [6, 7] and experimental [27, 36] studies. In the 195 datasets obtained from the 13 animals (Table 2), the coefficient of determination (R^2) between PCWP and $\text{PVP} \cdot S_T/S_M$ ($R^2 = 0.59$, Fig. 4a) was significantly higher than that between PCWP and CVP ($R^2 = 0.21$) ($P < 0.01$), but was significantly lower than that between PCWP and $\text{CVP} \cdot S_T/S_M$ ($R^2 = 0.78$) ($P < 0.01$) (data not shown). Taken all these together, $\text{PVP} \cdot S_T/S_M$ may not be a perfect, but reasonably reliable alternative to $\text{CVP} \cdot S_T/S_M$.

In clinical practice, physicians estimate CVP noninvasively by visual inspection of jugular pulsation [8], or by echocardiographic examination of cardiovascular dimensions [37, 38]. Clinical evaluation is needed to determine whether echocardiographic measurements of S_T/S_M in conjunction with the noninvasive estimation of CVP can be used to predict PCWP.

Potential sources of error of our technique

The diagnostic accuracy of our technique in the prediction of PCWP may be jeopardized when the assumptions in our theory (see “Materials and methods”) are not met. We assume equality of the stroke volumes of RV and LV. In mitral or tricuspid regurgitation, however, the stroke volumes of RV and LV are not equal owing to the presence of various degrees of regurgitant fraction. Some of the HF animals in this study showed mild to moderate degree of tricuspid and/or mitral regurgitation. We also assume a linear relationship between ventricular filling pressure and end-diastolic ventricular volume (Eqs. 5 and 6 in “Materials and methods”). This is not necessary valid especially in LV. The relationship between PCWP and LV end-diastolic ventricular volume can be regarded as linear at low pressures, but approximates curvilinear at high pressures [25, 39].

Restrictive LV filling patterns, a finding known to indicate clinical severity of HF, were also observed in some ALHF and CHF dogs in this study (Fig. 2a, c) [40]. The restrictive LV filling patterns are associated with diastolic ventricular interaction [41]. The direct inter-ventricular interaction is not considered in our theoretical analysis, which might affect the reliability of our technique.

The relation between PCWP and $\text{CVP} \cdot S_T/S_M$, or between PCWP and $\text{PVP} \cdot S_T/S_M$ may vary between subjects. Indeed, linear regression analysis between PCWP and $\text{CVP} \cdot S_T/S_M$ within individual animals indicated that the slope of the regression line varied from 0.6 to 1.7 among the 16 animals (data not shown). Furthermore, the relations

may be modified by the cardiac conditions. PCWP in CHF was higher than that in ALHF, while $CVP \cdot S_T/S_M$ (or $PVP \cdot S_T/S_M$) in ALHF was higher than that in CHF (Tables 1, 2).

S_T and S_M were recorded only at a single site on the tricuspid annulus and on the mitral annulus, respectively. S_T and S_M thus obtained might not completely reflect global RV and LV function, respectively, because ARHF and ALHF model created in this study possibly had regional myocardial dysfunction [14, 19, 21, 28].

All these might more or less introduce errors in the prediction of PCWP by our technique. However, it is fair to say that even with these potential sources of errors, our technique have enabled us to predict PCWP with acceptable degree of diagnostic accuracy.

Study limitations

The mongrel dogs used in this study were much smaller than human adults, and were anesthetized during data recordings. For validation purpose, we pooled the data of NC animals with the data of animals with very different HF conditions to obtain wide distribution of PCWP, and changed the relation between CVP and PCWP over a wide range. However, this pooled population might be irrelevant in routine clinical practice of HF management.

Clinical relevance of the canine HF models used in this study is limited. The difference between coronary micro-embolization in healthy dogs to create ALHF and the epicardial coronary occlusion in patients is evident. Tachycardia-induced CHF in dogs and human end-stage HF are different with respect to the time scales of development and persistence of failure. The values of E/E_a noted in HF dogs (Table 2) are smaller than those observed in HF patients [3–7, 42], although they are similar to those reported previously in HF dogs [36]. The E_a values in HF dogs (Table 2) [36] are larger than those in HF patients [3, 42], suggesting that the canine HF models might not have severe diastolic dysfunction observed in HF patients. In relation to this, lack of a diastolic HF model, characterized by HF with preserved EF, may be another limitation of this study. Diastolic HF accounts for approximately 50 % of HF cases [43].

Echocardiography assessment may be affected by inter- and intra-operator variability [44]. In this study, placement of the ultrasound probe on the dog's chest wall and acquisition of Doppler data were conducted by one investigator (KU). Hence, it was impossible to analyze inter- and intra-operator variability of $CVP \cdot S_T/S_M$ or $PVP \cdot S_T/S_M$.

Further studies are required to address these issues, and to extensively evaluate whether or not our technique can reliably predict PCWP in conscious/anesthetized patients with various types of HF.

Conclusions

CVP corrected by the relationship between RV and LV functions ($CVP \cdot S_T/S_M$) reliably predicts abnormal elevation and serial changes of PCWP in canine models of various types of HF. $PVP \cdot S_T/S_M$ may be used as a minimally invasive alternative to $CVP \cdot S_T/S_M$. The present results warrant further research and development of this technique for future clinical application.

Acknowledgments This study was supported by Grant-in-Aid for Scientific Research (C-24500565, C-24591087) from the Ministry of Education, Culture, Sports, Science and Technology, and by Intramural Research Fund (22-1-5, 25-2-1) for Cardiovascular Diseases of National Cerebral and Cardiovascular Center.

Conflict of interest The authors declare no conflict of interest.

References

- Solomonica A, Burger AJ, Aronson D (2013) Hemodynamic determinants of dyspnea improvement in acute decompensated heart failure. *Circ Heart Fail* 6:53–60
- National Heart, Lung, and Blood Institute Acute Respiratory Distress Syndrome (ARDS) Clinical Trials Network, Wheeler AP, Bernard GR, Thompson BT, Schoenfeld D, Wiedemann HP, deBoisblanc B, Connors AF Jr, Hite RD, Harabin AL (2006) Pulmonary-artery versus central venous catheter to guide treatment of acute lung injury. *N Engl J Med* 354:2213–2224
- Nagueh SF, Middleton KJ, Kopelen HA, Zoghbi WA, Quiñones MA (1997) Doppler tissue imaging: a noninvasive technique for evaluation of left ventricular relaxation and estimation of filling pressures. *J Am Coll Cardiol* 30:1527–1533
- Ommen SR, Nishimura RA, Appleton CP, Miller FA, Oh JK, Redfield MM, Tajik AJ (2000) Clinical utility of Doppler echocardiography and tissue Doppler imaging in the estimation of left ventricular filling pressures: a comparative simultaneous Doppler-catheterization study. *Circulation* 102:1788–1794
- Masutani S, Saiki H, Kurishima C, Kuwata S, Tamura M, Senzaki H (2013) Assessment of ventricular relaxation and stiffness using early diastolic mitral annular and inflow velocities in pediatric patients with heart disease. *Heart Vessels*. doi:10.1007/s00380-013-0422-2
- Mullens W, Borowski AG, Curtin RJ, Thomas JD, Tang WH (2009) Tissue Doppler imaging in the estimation of intracardiac filling pressure in decompensated patients with advanced systolic heart failure. *Circulation* 119:62–70
- Bhella PS, Pacini EL, Prasad A, Hastings JL, Adams-Huet B, Thomas JD, Grayburn PA, Levine BD (2011) Echocardiographic indices do not reliably track changes in left-sided filling pressure in healthy subjects or patients with heart failure with preserved ejection fraction. *Circ Cardiovasc Imaging* 4:482–489
- Butman SM, Ewy GA, Standen JR, Kern KB, Hahn E (1993) Bedside cardiovascular examination in patients with severe chronic heart failure: importance of rest or inducible jugular venous distension. *J Am Coll Cardiol* 22:968–974
- Drazner MH, Prasad A, Ayers C, Markham DW, Hastings J, Bhella PS, Shibata S, Levine BD (2010) The relationship of right- and left-sided filling pressures in patients with heart failure and a preserved ejection fraction. *Circ Heart Fail* 3:202–206
- Forrester JS, Diamond G, McHugh TJ, Swan HJ (1971) Filling pressures in the right and left sides of the heart in acute

- myocardial infarction. A reappraisal of central-venous-pressure monitoring. *N Engl J Med* 285:190–193
11. Campbell P, Drazner MH, Kato M, Lakdawala N, Palardy M, Nohria A, Stevenson LW (2011) Mismatch of right- and left-sided filling pressures in chronic heart failure. *J Card Fail* 17:561–568
 12. Terrovitis JV, Kapelios CJ, Sainis G, Ntalianis A, Kaldara E, Sousounis V, Vakrou S, Michelinakis N, Anagnostou D, Margari Z, Nanas JN (2013) Elevated left ventricular filling pressures can be estimated with accuracy by a new mathematical model. *J Heart Lung Transpl* 32:511–517
 13. Berglund E (1954) Ventricular function. VI. Balance of left and right ventricular output: relation between left and right atrial pressures. *Am J Physiol* 178:381–386
 14. Uemura K, Sugimachi M, Kawada T, Kamiya A, Jin Y, Kashi-hara K, Sunagawa K (2004) A novel framework of circulatory equilibrium. *Am J Physiol Heart Circ Physiol* 286:H2376–H2385
 15. Wahl A, Praz F, Schwerzmann M, Bonel H, Koestner SC, Hullin R, Schmid JP, Stuber T, Delacrétaiz E, Hess OM, Meier B, Seiler C (2011) Assessment of right ventricular systolic function: comparison between cardiac magnetic resonance derived ejection fraction and pulsed-wave tissue Doppler imaging of the tricuspid annulus. *Int J Cardiol* 151:58–62
 16. Meluzin J, Spinarová L, Bakala J, Toman J, Krejčí J, Hude P, Kára T, Soucek M (2001) Pulsed Doppler tissue imaging of the velocity of tricuspid annular systolic motion; a new, rapid, and non-invasive method of evaluating right ventricular systolic function. *Eur Heart J* 22:340–348
 17. Hori Y, Ukai Y, Hoshi F, Higuchi S (2008) Volume loading-related changes in tissue Doppler images derived from the tricuspid valve annulus in dogs. *Am J Vet Res* 69:33–38
 18. Yuda S, Inaba Y, Fujii S, Kokubu N, Yoshioka T, Sakurai S, Nishizato K, Fujii N, Hashimoto A, Uno K, Nakata T, Tsuchihashi K, Miura T, Ura N, Natori H, Shimamoto K (2006) Assessment of left ventricular ejection fraction using long-axis systolic function is independent of image quality: a study of tissue Doppler imaging and m-mode echocardiography. *Echocardiography* 23:846–852
 19. Alam M, Wardell J, Andersson E, Samad BA, Nordlander R (2000) Effects of first myocardial infarction on left ventricular systolic and diastolic function with the use of mitral annular velocity determined by pulsed wave Doppler tissue imaging. *J Am Soc Echocardiogr* 13:343–352
 20. Seo JS, Kim DH, Kim WJ, Song JM, Kang DH, Song JK (2010) Peak systolic velocity of mitral annular longitudinal movement measured by pulsed tissue Doppler imaging as an index of global left ventricular contractility. *Am J Physiol Heart Circ Physiol* 298:H1608–H1615
 21. Uemura K, Kawada T, Sunagawa K, Sugimachi M (2011) Peak systolic mitral annulus velocity reflects the status of ventricular-arterial coupling—theoretical and experimental analyses. *J Am Soc Echocardiogr* 24:582–591
 22. Orient JM (2009) Sapira's art and science of bedside diagnosis. Lippincott Williams & Wilkins, Philadelphia, pp 401–402
 23. Amar D, Melendez JA, Zhang H, Dobres C, Leung DH, Padilla RE (2001) Correlation of peripheral venous pressure and central venous pressure in surgical patients. *J Cardiothorac Vasc Anesth* 15:40–43
 24. Sobol I, Barst RJ, Nichols K, Widlitz A, Horn E, Bergmann SR (2004) Correlation between right ventricular ejection fraction obtained with gated equilibrium blood pool spect imaging and right atrial pressure in patients with primary pulmonary hypertension. *J Nucl Cardiol* 11:S25–S26
 25. Greene ES, Gerson JI (1986) One versus two MAC halothane anesthesia does not alter the left ventricular diastolic pressure–volume relationship. *Anesthesiology* 64:230–237
 26. Uemura K, Kawada T, Inagaki M, Sugimachi M (2013) A minimally invasive monitoring system of cardiac output using aortic flow velocity and peripheral arterial pressure profile. *Anesth Analg* 116:1006–1017
 27. Jacques DC, Pinsky MR, Severyn D, Gorcsan J 3rd (2004) Influence of alterations in loading on mitral annular velocity by tissue Doppler echocardiography and its associated ability to predict filling pressures. *Chest* 126:1910–1918
 28. Zwissler B, Forst H, Messmer K (1990) Acute pulmonary microembolism induces different regional changes in preload and contraction pattern in canine right ventricle. *Cardiovasc Res* 24:285–295
 29. Shinbane JS, Wood MA, Jensen DN, Ellenbogen KA, Fitzpatrick AP, Scheinman MM (1997) Tachycardia-induced cardiomyopathy: a review of animal models and clinical studies. *J Am Coll Cardiol* 29:709–715
 30. Zou KH, O'Malley AJ, Mauri L (2007) Receiver-operating characteristic analysis for evaluating diagnostic tests and predictive models. *Circulation* 115:654–657
 31. Skalska H, Freylich V (2006) Web-bootstrap estimate of area under ROC curve. *Aust J Stat* 35:325–330
 32. Swets JA (1988) Measuring the accuracy of diagnostic systems. *Science* 240:1285–1293
 33. Bruhl SR, Chahal M, Khouri SJ (2011) A novel approach to standard techniques in the assessment and quantification of the interventricular systolic relationship. *Cardiovasc Ultrasound* 9:42
 34. Gromadziński L, Targoński R (2007) The role of tissue colour Doppler imaging in diagnosis of segmental pulmonary embolism in congestive heart failure patients. *Kardiol Pol* 65:1433–1439
 35. Drazner MH, Velez-Martinez M, Ayers CR, Reimold SC, Thibodeau JT, Mishkin JD, Mammen PP, Markham DW, Patel CB (2013) Relationship of right- to left-sided ventricular filling pressures in advanced heart failure: insights from the ESCAPE trial. *Circ Heart Fail* 6:264–270
 36. Schober KE, Stern JA, DaCunha DN, Pedraza-Toscano AM, Shemanski D, Hamlin RL (2008) Estimation of left ventricular filling pressure by Doppler echocardiography in dogs with pacing-induced heart failure. *J Vet Intern Med* 22:578–585
 37. Beigel R, Cercek B, Luo H, Siegel RJ (2013) Noninvasive evaluation of right atrial pressure. *J Am Soc Echocardiogr* 26:1033–1042
 38. Hattori H, Minami Y, Mizuno M, Yumino D, Hoshi H, Arashi H, Nuki T, Sashida Y, Higashitani M, Serizawa N, Yamada N, Yamaguchi J, Mori F, Shiga T, Hagiwara N (2013) Differences in hemodynamic responses between intravenous carperitide and nicorandil in patients with acute heart failure syndromes. *Heart Vessels* 28:345–351
 39. Glantz SA, Kernoff RS (1975) Muscle stiffness determined from canine left ventricular pressure–volume curves. *Circ Res* 37:787–794
 40. Solomon SB, Nikolic SD, Glantz SA, Yellin EL (1998) Left ventricular diastolic function of remodeled myocardium in dogs with pacing-induced heart failure. *Am J Physiol* 274:H945–H954
 41. Atherton JJ, Moore TD, Thomson HL, Frenneaux MP (1998) Restrictive left ventricular filling patterns are predictive of diastolic ventricular interaction in chronic heart failure. *J Am Coll Cardiol* 31:413–418
 42. Takaya Y, Taniguchi M, Sugawara M, Nobusada S, Kusano K, Akagi T, Ito H (2013) Evaluation of exercise capacity using wave intensity in chronic heart failure with normal ejection fraction. *Heart Vessels* 28:179–187
 43. Lam CS, Donal E, Kraigher-Krainer E, Vasan RS (2011) Epidemiology and clinical course of heart failure with preserved ejection fraction. *Eur J Heart Fail* 13:18–28
 44. Magda SL, Ciobanu AO, Florescu M, Vinereanu D (2013) Comparative reproducibility of the noninvasive ultrasound methods for the assessment of vascular function. *Heart Vessels* 28:143–150

Chronic vagal nerve stimulation improves baroreflex neural arc function in heart failure rats

Toru Kawada, Meihua Li, Can Zheng, Shuji Shimizu, Kazunori Uemura, Michael J. Turner, Hiromi Yamamoto and Masaru Sugimachi

J Appl Physiol 116:1308-1314, 2014. First published 27 March 2014;
doi:10.1152/jappphysiol.00140.2014

You might find this additional info useful...

This article cites 27 articles, 12 of which can be accessed free at:
</content/116/10/1308.full.html#ref-list-1>

Updated information and services including high resolution figures, can be found at:
</content/116/10/1308.full.html>

Additional material and information about *Journal of Applied Physiology* can be found at:
<http://www.the-aps.org/publications/jappph>

This information is current as of August 18, 2014.

Chronic vagal nerve stimulation improves baroreflex neural arc function in heart failure rats

Toru Kawada,¹ Meihua Li,¹ Can Zheng,¹ Shuji Shimizu,¹ Kazunori Uemura,¹ Michael J. Turner,¹ Hiromi Yamamoto,² and Masaru Sugimachi¹

¹Department of Cardiovascular Dynamics, National Cerebral and Cardiovascular Center, Osaka, Japan; and ²Division of Cardiology, Department of Medicine, Faculty of Medicine, Kinki University, Osaka, Japan

Submitted 12 February 2014; accepted in final form 25 March 2014

Kawada T, Li M, Zheng C, Shimizu S, Uemura K, Turner MJ, Yamamoto H, Sugimachi M. Chronic vagal nerve stimulation improves baroreflex neural arc function in heart failure rats. *J Appl Physiol* 116: 1308–1314, 2014. First published March 27, 2014; doi:10.1152/jappphysiol.00140.2014.—We tested whether 6-wk vagal stimulation (VS) treatment improved open-loop baroreflex function in rats after myocardial infarction (MI). The following three groups of Sprague-Dawley rats were examined: normal control (NC, $n = 9$), MI with no treatment (MI-NT, $n = 8$), and MI treated with VS (MI-VS, $n = 7$). Under anesthesia, a stepwise input ranging from 60 to 180 mmHg was imposed on isolated carotid sinus baroreceptor regions, while the responses in splanchnic sympathetic nerve activity (SNA) and arterial pressure (AP) were measured. The response range of percent SNA was greater in the MI-VS than in the MI-NT group ($63.8 \pm 4.9\%$ vs. $33.1 \pm 3.8\%$, $P < 0.01$). The slope of the AP response to percent SNA was not different between the MI-VS and MI-NT groups (0.611 ± 0.076 vs. 0.781 ± 0.057 mmHg/%). The difference in the response range of AP between the MI-VS and MI-NT groups did not reach statistical significance (40.7 ± 6.2 vs. 26.4 ± 3.5 mmHg). In conclusion, the 6-wk VS treatment significantly improved the baroreflex control of SNA, but the effect was limited for the baroreflex total-loop function due to the lack of significant improvement in the AP response to percent SNA.

carotid sinus baroreflex; open-loop analysis; sympathetic nerve activity; myocardial infarction

PROGRESSION of heart failure is associated with autonomic imbalance characterized by sympathetic overactivity and vagal withdrawal (5, 11). Although mechanisms involved in the autonomic imbalance are not completely elucidated, impaired arterial and cardiac baroreflexes are important contributing factors (1, 3, 26). To correct the autonomic imbalance, vagal stimulation (VS) has been proposed as a therapeutic approach for heart failure (12, 14, 20, 23–25, 29). In a rat model of chronic heart failure following myocardial infarction (MI), 6-wk VS has been shown to improve the survival rate (14). However, whether the VS treatment improves the impaired arterial baroreflex function in MI-induced heart failure remains undetermined. A close association between the dysfunction of the autonomic nervous system and the derangement of the immune system is postulated in the pathophysiology of heart failure (5). Systemic inflammatory responses are observed in heart failure, and pharmacological vagal activation (13) or electrical VS (29) can reduce the inflammatory responses. The VS treatment may ameliorate inflammation in the heart and reduce pathological afferent signals from the damaged heart to the central nervous system. Because cardiac sympathetic afferent activation

inhibits the baroreflex control of sympathetic nerve activity (SNA) in heart failure (3), it is postulated that the VS treatment may improve baroreflex function. To gain an insight into the treatment mechanism of VS, the present study examined the effects of 6-wk VS on the arterial baroreflex function in MI rats.

The arterial baroreflex system may be analyzed by dividing it into two principal subsystems: a neural arc subsystem from pressure input to efferent SNA, and a peripheral arc subsystem from SNA to arterial pressure (AP) (16, 18). Under normal physiological conditions, an increase in AP suppresses SNA via the arterial baroreflex, which resultantly decreases AP, and vice versa. This closed-loop feedback operation makes it difficult to separately quantify the characteristics of the neural and peripheral arc subsystems. To circumvent the problem, the present study employed an isolated carotid sinus preparation by which the open-loop baroreflex function can be assessed over the entire operating range of the carotid sinus baroreflex (7–9, 27).

MATERIALS AND METHODS

Animal care was provided in strict accordance with the *Guiding Principles for the Care and Use of Animals in the Field of Physiological Sciences*, approved by the Physiological Society of Japan. All protocols were reviewed and approved by the Animal Subject Committee of National Cerebral and Cardiovascular Center. The following groups of Sprague-Dawley rats were examined: normal control (NC), MI with no treatment (MI-NT), and MI with VS treatment (MI-VS).

Creation of myocardial infarction and device implantation. For the MI-NT and MI-VS groups, the left coronary artery was ligated under halothane anesthesia in 8-wk male rats (14). One week later, the rats in the MI-VS group underwent a second surgery for implanting a radiocontrolled pulse generator (ISE1010C, Unimec) to stimulate the right vagus and an electrocardiogram transmitter (TA10CA-F10, Data Science International) to monitor heart rate (HR). The total weight of the implanted devices was 17 g. This value was subtracted in the measurement of body weight in the MI-VS group. The VS treatment was started from 1 wk after the device implantation (i.e., 2 wk after the MI induction). The right vagus was stimulated using a rectangular pulse of 0.2-ms duration at 20 Hz for 10 s every minute according to our previous study (14). The intensity of VS was adjusted in each rat to reduce HR by 20–30 beats/min. The VS treatment was continued for 6 wk until the day of the acute experiment described below. The VS was ceased when the rat was removed out of the cage for the acute baroreflex study. Because the intraperitoneal anesthesia took ~30 min to develop its sufficient effect and the preparation for venous and arterial lines took 10–20 min, an acute effect of VS might have been lost before the measurement of baseline AP and HR.

Acute baroreflex study. Each rat was anesthetized with an intraperitoneal injection (2 ml/kg) of a mixture of urethane (250 mg/ml) and α -chloralose (40 mg/ml), and mechanically ventilated with oxygen-supplied room air. Anesthesia was maintained by a continuous intravenous infusion of a diluted solution of the above anesthetic mixture from the right femoral vein. An arterial catheter was inserted

Address for reprint requests and other correspondence: T. Kawada, Dept. of Cardiovascular Dynamics, National Cerebral and Cardiovascular Center, 5-7-1 Fujishirodai, Suita, Osaka 565-8565, Japan (e-mail: torukawa@ncvc.go.jp).

Table 1. Number of animals used in the acute baroreflex study

	NC	MI-NT	MI-VS
Total number	9	15	10
Death during operation	0	2	0
Small biventricular weight ^a	N/A	2	1
Diminished baroreflex function ^b	0	3	0
Electrode failure ^c	N/A	N/A	2
Included in final data analysis	9	8	7

NC, normal control; MI-NT, myocardial infarction with no treatment; MI-VS, myocardial infarction treated with vagal stimulation; N/A, not applicable. ^aSmall biventricular weight was defined as normalized biventricular weight of less than 2.2 g/kg, which suggested insufficient myocardial infarction to induce cardiac remodeling. ^bDiminished baroreflex function was defined as a magnitude of arterial pressure response of less than 10 mmHg during the input pressure change from 60 to 180 mmHg. Because some litters of rats do not tolerate the bilateral carotid occlusion, we cannot determine whether the diminished baroreflex was truly attributable to the effect of myocardial infarction. Hence the data from these 3 rats were excluded from the final data analysis. This exclusion does not affect our main conclusion because including the 3 rats would only exaggerate the impaired baroreflex function in the MI-NT group. ^cElectrode failure was defined as the lack of periodic bradycardia during 10 s on and 50 s off vagal stimulation, which suggested broken lead wire. Although nerve injury may also result in the lack of bradycardia, discoloration of the nerve in the cuff electrode was not observed by macroscopic inspection.

into the right femoral artery to measure AP and HR. Another catheter was inserted into the left femoral vein to measure central venous pressure. Body temperature of the animal was maintained at ~38°C using a heating pad and a lamp.

A postganglionic branch of the splanchnic sympathetic nerve was exposed retroperitoneally, and a pair of stainless steel wire electrodes (Bioflex wire, AS633, Cooner Wire) was attached to the nerve. This nerve was selected as representing the sympathetic outflow because the splanchnic vascular bed contributes to approximately one-third of the change in the total vascular conductance in the AP regulation (17). This nerve is thicker than the often-used renal sympathetic nerve and was easy to locate even when the surrounding tissue was edematous in the MI rats. The nerve and electrodes were covered with silicone glue (Kwik-Sil, World Precision Instruments). A preamplified nerve signal was band-pass filtered at 150–1,000 Hz, and then full-wave rectified and low-pass filtered at a cut-off frequency of 30 Hz using analog circuits. A ganglionic blocker hexamethonium bromide (60 mg/kg) was given intravenously at the end of the experiment to confirm the disappearance of SNA and to measure the noise level.

The aortic depressor nerves and the vagal nerves were sectioned, and carotid sinus baroreceptor regions were isolated from systemic circulation bilaterally (19, 21). The isolated carotid sinuses were filled with warmed Ringer's solution through catheters inserted into the common carotid arteries. Carotid sinus pressure (CSP) was controlled using a servocontrolled piston pump. Heparin sodium (100 U/kg) was given intravenously to prevent blood coagulation.

Protocols. After completing the above surgery, the baroreflex-mediated AP response was monitored for more than 30 min. The rat was excluded from the final data analysis in the event that the reflex response to CSP was progressively diminished within this stabilization period. Possible causes for the deterioration include surgical damage to the carotid sinus nerves and brain ischemia due to the bilateral carotid occlusion. Although the vertebral arteries were kept patent, some litters of rats do not tolerate the bilateral carotid occlusion. We occasionally experience diminished baroreflex function even in normal rats. In the present study, three rats assigned to the MI-NT group were excluded from the final data analysis because of diminished baroreflex function (Table 1). This exclusion does not affect our main conclusion, because including the three rats would only exaggerate the impaired baroreflex function in the MI-NT group.

After the stabilization, CSP was decreased to 60 mmHg for 4 min, and then increased stepwise from 60 to 180 mmHg in increments of 20 mmHg every minute (8). The data obtained from two consecutive stepwise CSP inputs were averaged for analysis.

Data analysis. The rats assigned to the MI-NT and MI-VS groups were excluded from the final data analysis when the normalized biventricular weight was less than 2.2 g/kg (based on the mean plus 1 SD of the NC group), because it indicated insufficient development of heart failure due to small MI (Table 1). On the other hand, two rats in the MI-NT group did not survive the acute baroreflex study due to severe heart failure (the normalized biventricular weights were 2.97 and 3.00 g/kg, respectively). Resultantly, 9 rats in the NC group, 8 rats in the MI-NT group and 7 rats in the MI-VS group were used for the final data analysis (Table 1).

Data were acquired at 1,000 Hz using a 16-bit analog-to-digital converter. Mean SNA, AP, and HR values were calculated at each CSP level by averaging the data during the last 10 s of each step. Because the absolute amplitude of SNA varied among animals depending on recording conditions, SNA was presented in percent values in each animal. The SNA value corresponding to the CSP level of 60 mmHg was assigned to 100%. The noise level after the hexamethonium administration was assigned to 0%.

The CSP-SNA, CSP-AP, and CSP-HR relationships approximated an inverse sigmoid curve and were quantified using a four-parameter logistic function as (10):

$$y = \frac{P_1}{1 + \exp[P_2(\text{CSP} - P_3)]} + P_4$$

where y denotes the output (SNA, AP, or HR); P_1 is the response range of y (i.e., the difference between the maximum and minimum values of y); P_2 is the slope coefficient; P_3 is the midpoint of the sigmoid curve on the CSP axis; and P_4 is the minimum value of y (i.e., the lower plateau of the sigmoid curve). The maximum gain or the maximum slope of the sigmoid curve was calculated as $P_1 P_2 / 4$.

The SNA-AP relationship approximated a straight line and was quantified using a linear regression as:

$$\text{AP} = P_a \text{SNA} + P_b$$

where P_a and P_b are the slope and intercept, respectively.

Statistical analysis. All data are presented as means and SE values. Each parameter was compared among NC, MI-NT, and MI-VS groups using one-way analysis of variance (ANOVA) followed by Tukey test for simultaneous multiple comparisons. Differences were considered significant when $P < 0.05$ (4).

RESULTS

As shown in Table 2, body weight was not different among the three groups. Biventricular weight was significantly heavier

Table 2. Body weight, biventricular weight, and baseline hemodynamics

	NC (n = 9)	MI-NT (n = 8)	MI-VS (n = 7)
Body wt, kg	0.486 ± 0.012	0.468 ± 0.013	0.462 ± 0.012
Biventricular wt, g	1.001 ± 0.023	1.292 ± 0.042†	1.289 ± 0.054†
Normalized biventricular wt, g/kg	2.06 ± 0.04	2.76 ± 0.08†	2.80 ± 0.11†
Central venous pressure, mmHg	1.52 ± 0.17	3.14 ± 0.30†	2.41 ± 0.16*
Mean arterial pressure, mmHg	126.6 ± 5.9	110.9 ± 5.8	115.0 ± 4.8
Heart rate, beats/min	408.6 ± 13.1	379.5 ± 12.6	380.1 ± 9.5

Values are means ± SE. NC, normal control; MI-NT, myocardial infarction with no treatment; MI-VS, myocardial infarction treated with vagal stimulation. * $P < 0.05$, † $P < 0.01$ vs. NC by Tukey test following one-way ANOVA.

in the MI-NT and MI-VS groups compared with the NC group. Central venous pressure, measured just after inserting arterial and venous catheters and before isolating baroreceptor regions, was higher in the MI-NT and MI-VS groups compared with the NC group. Mean AP and HR under the baseline conditions did not differ among the three groups.

Typical time series obtained from the NC, MI-NT, and MI-VS rats are shown in Fig. 1. The gray lines in the AP and HR signals represent 200-Hz resampled data. The gray lines in the SNA signals represent 10-Hz resampled data. The black lines in the SNA, AP, and HR signals indicate 2-s moving averaged data. The increase in CSP decreased SNA, AP, and HR in all groups, but the baroreflex responses in the MI-NT rat were smaller than those in the NC and MI-VS rats.

Static characteristics of the baroreflex neural arc obtained from the NC, MI-NT, and MI-VS groups are illustrated in Fig. 2, A–C. The response range of percent SNA was significantly narrower in the MI-NT group than in the NC group and was significantly wider in the MI-VS than in the MI-NT group (Fig. 2D). Differences in the maximum slope among the three groups were not statistically significant (Fig. 2E). The midpoint pressure was significantly lower in the MI-NT group than in the NC group, but the difference was not observed between the NC and MI-VS group (Fig. 2F). Changes in the lower plateau of SNA were reciprocal to those in the response range of SNA because the maximum SNA was assigned to 100% in each animal (Fig. 2G).

Static characteristics of the baroreflex peripheral arc approximated a straight line in all of the NC, MI-NT, and MI-VS

groups (Fig. 3, A–C). The slope was significantly smaller in the MI-NT and MI-VS groups than in the NC group (Fig. 3D). The slope did not differ significantly between the MI-NT and MI-VS groups. The intercept tended to be higher in the MI-VS than in the NC group, but the difference in the intercept was not statistically significant among the three groups (Fig. 3E).

Static characteristics of the baroreflex total loop obtained from the NC, MI-NT, and MI-VS groups are summarized in Fig. 4, A–C. The response range of AP was significantly narrower in the MI-NT and MI-VS groups than in the NC group (Fig. 4D). The maximum gain was significantly smaller in the MI-NT group than in the NC group, but was not significantly different between the NC and MI-VS groups (Fig. 4E). The midpoint pressure and the lower plateau did not differ significantly among the three groups (Fig. 4, F and G).

Static characteristics of the baroreflex control of HR obtained from the NC, MI-NT, and MI-VS groups are depicted in Fig. 5, A–C. The response range of HR was significantly narrower in the MI-NT group than in the NC and MI-VS groups (Fig. 5D). The maximum slope of the HR response was significantly greater in the MI-VS group than in the MI-NT group (Fig. 5E). The midpoint pressure and the lower plateau did not differ significantly among the three groups (Fig. 5, F and G).

DISCUSSION

The present results demonstrated that the 6-wk VS treatment improved the ability of the carotid sinus baroreflex to suppress

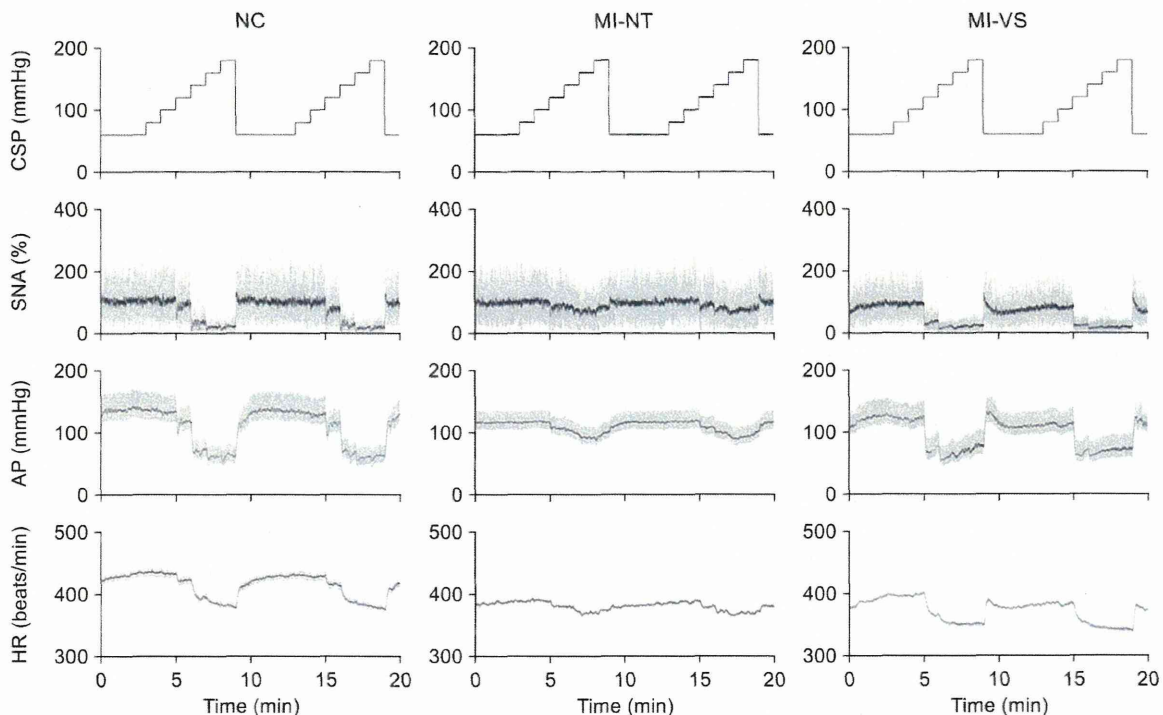


Fig. 1. Typical experimental recordings of carotid sinus pressure (CSP), sympathetic nerve activity (SNA), arterial pressure (AP), and heart rate (HR) obtained from rats of normal control (NC), myocardial infarction with no treatment (MI-NT), and myocardial infarction with vagal stimulation (MI-VS). The gray lines in the AP and HR plots represent 200-Hz resampled signals. The gray lines in the SNA plots represent 10-Hz resampled signals. The black lines in the SNA, AP, and HR plots represent 2-s moving averaged signals. CSP was changed from 60 to 180 mmHg with an increment of 20 mmHg every minute. SNA, AP, and HR were decreased in response to the increase in CSP. The baroreflex responses were smaller in the MI-NT rat than in the NC and MI-VS rats.

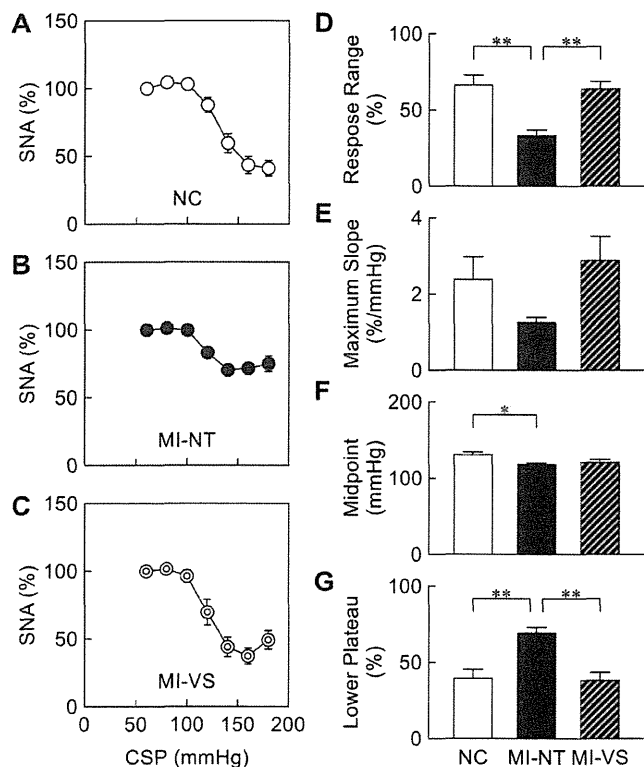


Fig. 2. Open-loop static characteristics of the baroreflex neural arc (SNA vs. CSP) obtained from the NC (A), MI-NT (B), and MI-VS (C) groups. The response range of percent SNA (D), maximum slope (E), midpoint (F), and lower plateau (G) derived from fitted sigmoid curves. Data are mean and SE values. $**P < 0.01$ and $*P < 0.05$ by Tukey test following one-way ANOVA.

percent SNA in the neural arc (Fig. 2D). On the other hand, the VS treatment did not affect the slope of the AP response to percent SNA in the peripheral arc (Fig. 3D). As a result, the VS treatment did not reveal statistically significant improvement in the response range of AP in the baroreflex total loop (Fig. 4D). No significant difference in the maximum gain between the NC and MI-VS groups may partly reflect an improvement of the baroreflex total-loop function (Fig. 4E).

Effects of VS treatment on the baroreflex neural arc. The response range of percent SNA was narrowed in the MI-NT group compared with the NC group (Fig. 2D), being consistent with our previous study that was performed in rats with longer duration of heart failure (100–200 days after MI) (8). The response range of percent SNA in the MI-VS group was nearly the same as that in the NC group. The improved neural arc function to suppress percent SNA may partly contribute to the sympathetic suppression induced by the VS treatment such as reduced plasma norepinephrine levels (14, 29). Because percent SNA is influenced by basal sympathetic discharge, the improved response range of percent SNA does not necessarily indicate the improved sympathetic control has physiological significance. However, because the VS treatment also increased the response range of HR in the MI-VS group compared with the MI-NT group (Fig. 5D), we speculate that VS might have actually improved the sympathetic control of target organs.

Several mechanisms are considered for the impaired baroreflex control of SNA in heart failure. Plasma angiotensin II levels are increased in heart failure, and VS can suppress the increased plasma angiotensin II levels (29). Angiotensin II can increase the maximum SNA without significantly affecting the response range of SNA in the baroreflex neural arc (7). Cardiac sympathetic afferent activation inhibits the baroreflex control of SNA via a mechanism associated with central angiotensin II (3). On the other hand, vagal afferent stimulation by phenylbiguanide can decrease the maximum SNA without significantly affecting the response range of SNA in the baroreflex neural arc (6). Because VS might have activated not only efferent but also afferent pathways in our study, the vagal afferent stimulation probably antagonized the sympathoexcitation such as that induced by angiotensin II. In addition, pharmacological vagal activation (13) or electrical VS (29) can reduce systemic inflammatory responses in heart failure, which may contribute to sympathetic suppression by reducing the pathological afferent signals from the heart. Aside from the systemic inflammation, increases in proinflammatory cytokines in the brain may also produce sympathoexcitation in heart failure (28). Although a link between the VS treatment and central anti-inflammation seems elusive, the presence of a cholinergic anti-inflammatory pathway (22) suggests a possibility that VS suppresses sympathetic overactivity through the anti-inflammatory mechanism in the central nervous system as well as in the heart.

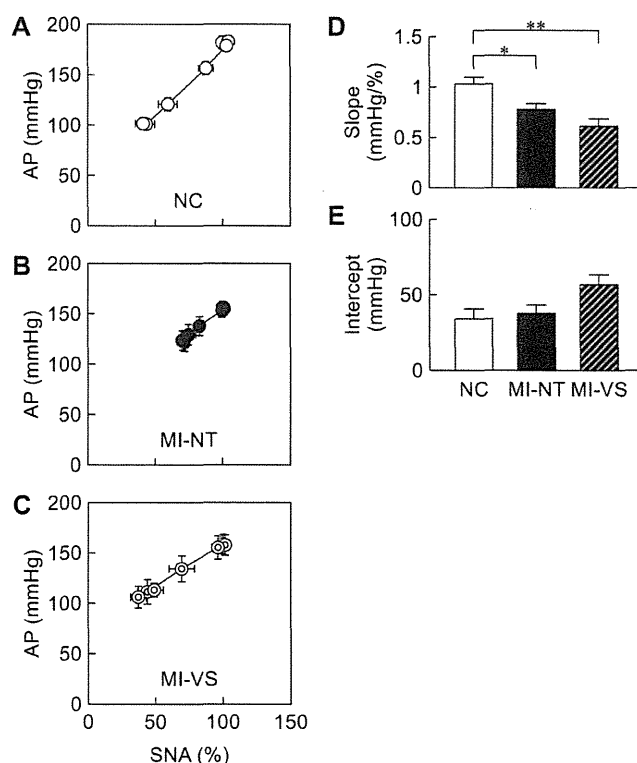


Fig. 3. Open-loop static characteristics of the baroreflex peripheral arc (AP vs. SNA) obtained from the NC (A), MI-NT (B), and MI-VS (C) groups. The slope (D) and intercept (E) derived from regression lines. Data are means and SE values. $**P < 0.01$ and $*P < 0.05$ by Tukey test following one-way ANOVA.

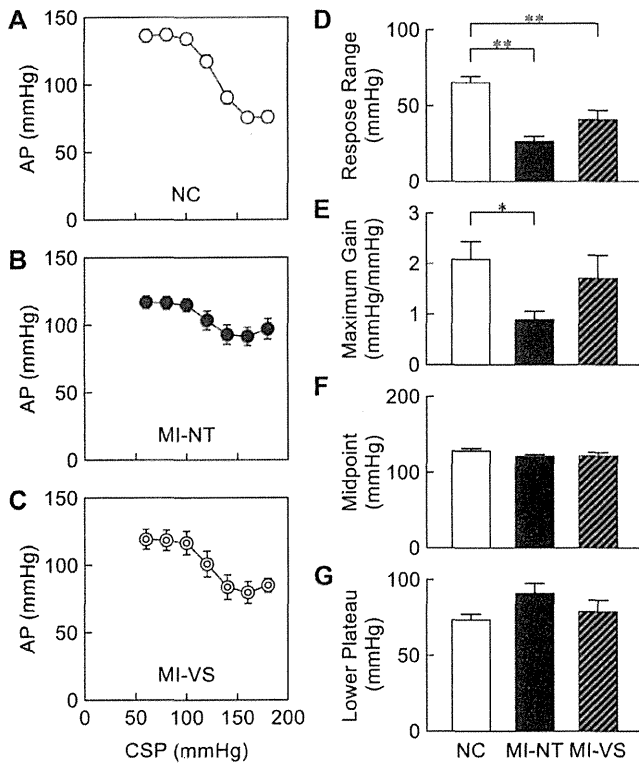


Fig. 4. Open-loop static characteristics of the baroreflex total loop (AP vs. CSP) obtained from the NC (A), MI-NT (B), and MI-VS (C) groups. The response range of AP (D), maximum gain (E), midpoint (F), and lower plateau (G) derived from fitted sigmoid curves. Data are means and SE values. $**P < 0.01$ and $*P < 0.05$ by Tukey test following one-way ANOVA.

Effects of VS treatment on the baroreflex peripheral arc. Open-loop static characteristics of the baroreflex peripheral arc approximated a straight line (Fig. 3, A–C). As has been reported in our previous study (8), the slope of the peripheral arc was significantly reduced in the MI-NT group compared with the NC group. Pump failure associated with MI may blunt the AP response to percent SNA. Regarding this point, Feng et al. (2) examined the AP response to preganglionic sympathetic nerve stimulation using pithed rats. In that study, the AP response is decreased in MI rats compared with control rats. They discussed that the pressor response in pithed rats mainly represented the vascular response because cardiac output did not change significantly in response to preganglionic sympathetic nerve stimulation. However, when cardiac output is reduced in the MI rats compared with the control rats, the same amount of changes in the peripheral vascular resistance would yield smaller AP response in the MI rats than in the control rats. In this sense, the contribution of pump failure to the decreased AP response may be inevitable.

The slope of the peripheral arc in the MI-VS group was not increased compared with the MI-NT group, indicating that the VS treatment had little effect on the sympathetic control of AP. While these results seem to be consistent with no significant effect of the VS treatment on the normalized biventricular weight (Table 2), we need to be cautious about the fact that the slope of the peripheral arc can be differently estimated depending on how SNA was expressed. For instance, if the absolute

maximum SNA is decreased in the MI-VS group compared with in the MI-NT group, the slope of the peripheral arc assessed by the AP response to the absolute change in SNA could be increased.

Effects of VS on the sympathetic HR control. Because the vagal nerves were sectioned bilaterally in the acute baroreflex study, the CSP-HR relationship represents the sympathetically mediated HR response (Fig. 5). The response range of HR was narrowed in the MI-NT group compared with the NC group, but it was nearly the same between the MI-VS and NC groups. In a previous study using canine heart failure induced by high-rate pacing, Zhang et al. (29) demonstrated that chronic VS improves the baroreflex sensitivity assessed by the RR interval response to a phenylephrine-induced AP increase. In that study, both the sympathetic and vagal limbs might have contributed to the RR interval response. In contrast, the present result indicates that the VS treatment may improve the HR response even in the absence of the vagal control of HR. Sustained sympathetic activation in heart failure results in downregulation and/or desensitization of β -adrenergic receptors (15). In addition to the improved SNA response to the CSP input, the VS treatment may correct the functionality of β -adrenergic signaling through sympathetic suppression and improve the sympathetically-mediated HR response in the MI-VS group compared with the MI-NT group.

Consideration of MI models. Our previous study indicates that the VS treatment prevents cardiac remodeling and ventricular

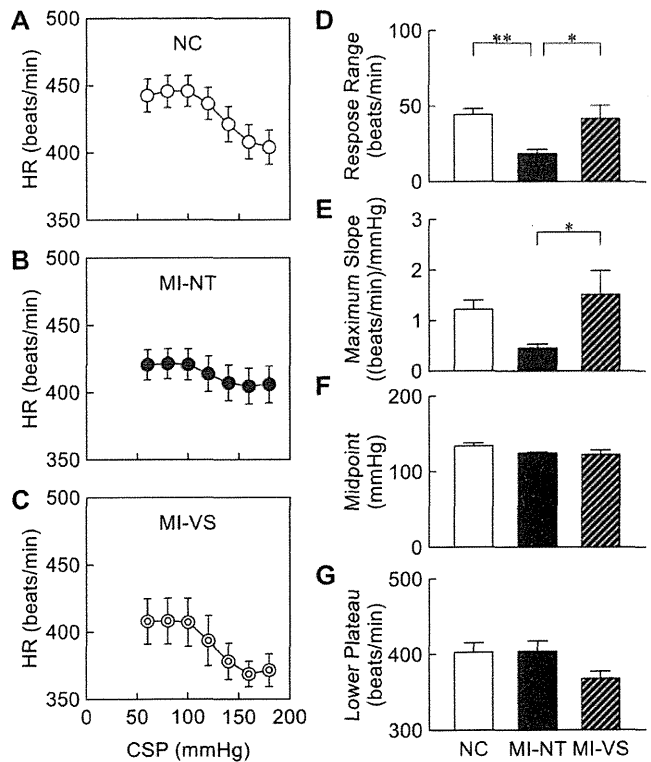


Fig. 5. Open-loop static characteristics of the baroreflex control of HR (HR vs. CSP) obtained from the NC (A), MI-NT (B), and MI-VS (C) groups. The response range of HR (D), maximum slope (E), midpoint (F), and lower plateau (G) derived from fitted sigmoid curves. Data are means and SE values. $**P < 0.01$ and $*P < 0.05$ by Tukey test following one-way ANOVA.

dysfunction in MI rats (14). In that study, normalized biventricular weight was 2.75 ± 0.25 g/kg in a treated group (CHF-VS) and 3.14 ± 0.22 g/kg in an untreated group (CHF-SS). In contrast, normalized biventricular weight was nearly the same between the MI-NT and MI-VS groups (Table 2), and both groups showed normalized biventricular weight similar to that in the CHF-VS group. One possible explanation for the discrepancy between the previous and present studies is the difference in the MI-NT and CHF-SS group characteristics as follows. In the previous study (14), a second surgery was performed for telemeter implantation and dummy stimulator implantation in the CHF-SS group. The second surgery and the weight burden of the implanted devices might have aggravated heart failure and promoted cardiac remodeling. In the present study, only MI was induced in the MI-NT group without the second surgery. Accordingly, heart failure might have been less severe in the MI-NT group than in the previous CHF-SS group.

Although performing the second surgery in the untreated MI group might have been a better protocol, it is confounded by another problem that the rat with too severe heart failure could not survive the acute baroreflex study (see APPENDIX for details). In this sense, there was unintentional bias as to the severity of heart failure in the MI-NT group. It may be worth noting that two rats in the MI-NT group but no rats in the MI-VS group were lost during the acute baroreflex study (Table 1).

Limitations. First, the baroreflex static characteristics were examined in anesthetized conditions. Because anesthesia affects autonomic nervous activities, the present results may not be directly extrapolated to interpret the baroreflex function in heart failure under conscious conditions. Second, we were unable to determine whether the VS treatment prevented worsening of the baroreflex neural arc function or restored the baroreflex neural arc function that had been worsened by heart failure before the initiation of the VS treatment. Further studies are required to elucidate the time course of the effects of the VS treatment on the baroreflex function. Finally, basal sympathetic discharge might have been increased in the MI-NT group compared with the NC group, and VS might have ameliorated the elevated sympathetic discharge in the MI-VS group. Our previous study (14) has demonstrated that chronic VS treatment reduces plasma norepinephrine concentration in MI-induced heart failure rats. Thus, if SNA was evaluated in absolute amplitude and/or frequency, the response range of SNA in the MI-NT group might become larger. In other words, the response range of the neural arc in the MI-NT group might be underestimated in Fig. 2, and the slope of the peripheral arc in the MI-NT group might be overestimated in Fig. 3. These points need to be taken into account when interpreting the data.

Conclusions. The 6-wk VS treatment significantly improved the ability of the carotid sinus baroreflex to reduce percent SNA. Because sympathetic overactivity promotes the progression of heart failure, the suppression of SNA may be beneficial for the improved prognosis of heart failure. On the other hand, the treatment effect of VS on the baroreflex total-loop function was limited due to the lack of significant improvement in the AP response to percent SNA.

APPENDIX

To address the effect of a second surgery in untreated MI rats, we performed an additional experiment, which included a sham operation on the right vagus and implantation of dummy devices in MI rats

(MI-SS). Eight rats survived until the day of the acute baroreflex study. One rat showed small normalized biventricular weight (<2.2 g/kg) and was excluded, and the remaining seven rats exhibited normalized biventricular weight of 3.05 ± 0.12 g/kg (mean \pm SE), confirming that a second surgery promoted cardiac remodeling compared with the MI-NT group. Among the seven rats, three rats died during the acute baroreflex study, and the remaining four rats exhibited normalized biventricular weight of 2.93 ± 0.13 g/kg. The problem with the MI-SS group was that rats with severe heart failure died during the acute baroreflex study, and we could not create a group of severe heart failure compared with the MI-NT group any further. As a reference, data obtained from the MI-SS group combined with other groups are depicted in Fig. 6. Statistical analyses were not performed due to the small number of successful baroreflex study in the MI-SS group ($n = 4$). The mean parameter values of the baroreflex total loop and the neural arc indicate that the baroreflex function in the MI-SS group was not worse than that in the MI-NT group.

GRANTS

This study was supported by Health and Labour Sciences Research Grants (H20-Katsudo-Shitei-007 and H21-Nano-Ippan-005) from the Ministry of Health, Labour and Welfare of Japan; by Grants-in-Aid for Scientific Research (JSPS KAKENHI Grant Nos. 23592319, 25350909); by a Grant-in-Aid for JSPS Fellows (JSPS KAKENHI Grant Number 23-01705); and by the Hiroshi and Aya Irisawa Memorial Award for Excellent Papers on Research in Circulation in The Journal of Physiological Sciences.

DISCLOSURES

No conflicts of interest, financial or otherwise, are declared by the author(s).

AUTHOR CONTRIBUTIONS

Author contributions: T.K. and M.S. conception and design of research; T.K., M.L., C.Z., and S.S. performed experiments; T.K. analyzed data; T.K., M.L., C.Z., S.S., K.U., M.J.T., and H.Y. interpreted results of experiments; T.K. prepared figures; T.K. and M.S. drafted manuscript; T.K. and M.S. edited and revised manuscript; T.K., M.L., C.Z., S.S., K.U., M.J.T., H.Y., and M.S. approved final version of manuscript.

REFERENCES

- DiBona GF, Sawin LL. Increased renal nerve activity in cardiac failure: arterial vs. cardiac baroreflex impairment. *Am J Physiol Regul Integr Comp Physiol* 268: R112–R116, 1995.
- Feng Q, Sun X, Lu X, Edvinsson L, Hedner T. Decreased responsiveness of vascular postjunctional α_1 -, α_2 -adrenoceptors and neuropeptide Y1 receptors in rats with heart failure. *Acta Physiol Scand* 166: 285–291, 1999.
- Gao L, Schultz HD, Patel KP, Zucker IH, Wang W. Augmented input from cardiac sympathetic afferents inhibits baroreflex in rats with heart failure. *Hypertension* 45: 1173–1181, 2005.
- Glantz SA. *Primer of Biostatistics* (5th ed.). New York: McGraw-Hill, 2002.
- Jankowska EA, Ponikowski P, Piepoli MF, Banasiak W, Anker SD, Poole-Wilson PA. Autonomic imbalance and immune activation in chronic heart failure. Pathophysiological links. *Cardiovasc Res* 70: 434–445, 2006.
- Kashihara K, Kawada T, Li M, Sugimachi M, Sunagawa K. Bezold-Jarisch reflex blunts arterial baroreflex via the shift of neural arc toward lower sympathetic nerve activity. *Jpn J Physiol* 54: 395–404, 2004.
- Kawada T, Kamiya A, Li M, Shimizu S, Uemura K, Yamamoto H, Sugimachi M. High levels of circulating angiotensin II shift the open-loop baroreflex control of splanchnic sympathetic nerve activity, heart rate and arterial pressure in anesthetized rats. *J Physiol Sci* 59: 447–455, 2009.
- Kawada T, Li M, Kamiya A, Shimizu S, Uemura K, Yamamoto H, Sugimachi M. Open-loop dynamic and static characteristics of the carotid sinus baroreflex in rats with chronic heart failure after myocardial infarction. *J Physiol Sci* 60: 283–298, 2010.
- Kawada T, Shimizu S, Li M, Kamiya A, Uemura K, Sata Y, Yamamoto H, Sugimachi M. Contrasting effects of moderate vagal stimulation on heart rate and carotid sinus baroreflex-mediated sympathetic arterial pressure regulation in rats. *Life Sci* 89: 498–503, 2011.